

Kelvin Waves in the Nonlinear Shallow Water Equations on the Sphere: Nonlinear Traveling Waves and the Corner Wave Bifurcation

John P. Boyd*

Cheng Zhou

Department of Atmospheric, Oceanic
and Space Science and Laboratory for Scientific Computation,
University of Michigan, 2455 Hayward Avenue, Ann Arbor MI 48109
jpboyd@engin.umich.edu;

May 27, 2009

Abstract

The Kelvin wave is the lowest eigenmode of Laplace's Tidal Equation and is widely observed in both the ocean and the atmosphere. In this work, we neglect mean currents and continuous stratification, but instead include the full effects of the earth's sphericity and the wave dispersion it induces in a one-and-a-half-layer model. In the first part, we derive a new asymptotic approximations for linear Kelvin waves on the sphere when ϵ (Lamb's parameter/nondimensional reciprocal depth) and integer zonal wavenumber s are of similar magnitude; we show that for large s , the Kelvin wave is equatorially-confined even in the barotropic limit ($\epsilon = 0$). In the second part, through a mix of perturbation theory and numerical computations using a Fourier/Newton iteration/continuation method, we show that for sufficiently small amplitude, there are Kelvin traveling waves (cnoidal waves). As the amplitude increases, the branch of traveling waves terminates in a so-called "corner wave" with a discontinuous first derivative. All waves larger than the corner wave evolve to fronts and break. The singularity is a point singularity in which only the longitudinal derivative is discontinuous. As we solve the nonlinear shallow water equations on the sphere with increasing ϵ ("Lamb's parameter"), dispersion weakens, the amplitude of the corner wave decreases rapidly, and the longitudinal profile of the corner wave narrows dramatically.

*

1 Introduction

This extended abstract is a summary of our recent article in the *Journal of Fluid Mechanics* [14] and also our earlier note on linear Kelvin waves in the *Journal of the Atmospheric Sciences* [15]. This extended abstract includes color versions of figures that were published in black-and-white.

The free oscillations of a layer of homogeneous fluid and uniform depth on a rotating, spherical earth are governed by a trio of nonlinear partial differential equations, the “Laplace Tidal Equations”, also known as the “nonlinear shallow water wave equations”. When linearized about a state of rest, these equations have eigenmodes which are commonly called “Hough” functions [25]. The slowest eastward-traveling wave has been given the special name of the “Kelvin wave”. This mode is the lowest latitudinal Hough function for each longitudinal wavenumber s . The nonlinear self-interaction of Kelvin waves has been studied by [1, 2, 5, 7],[17], [29], [34, 35], [24], [18], [20], [28], [22], [30]. In spite of this work, there are still significant gaps in both linear and nonlinear theory. Some of the linear lacunae have recently been filled by [12] and [15].

The nonlinear shallow water wave equations also describe the baroclinic mode of a two-layer model in the limit that the lower layer depth is infinite, in which case motion is confined to the upper layer, a so-called “one-and-a-half-layer” model (Gill, 1982). (This is a decent first approximation to the ocean, especially in the tropics.) The only modification is that the actual mean depth is replaced by the “equivalent depth”, which is the product of the mean depth with the fractional density difference between the two layers (Pedlosky, 1987). As explained in [29] and other references cited there, the shallow water equations also model the baroclinic modes of a continuously stratified fluid as first observed by G. I. Taylor seventy-five years ago; the main effect of continuous stratification is to slightly weaken the nonlinearity because of coupling between different vertical modes.

We extended the existing nonlinear shallow water equations theory of the Kelvin wave in a couple of ways. First, instead of using the equatorial beta-plane, which corresponds to the limit of a very thin ocean, we explicitly included the effects of the earth’s sphericity and finite depth (i. e., finite “Lamb’s parameter”). We then derived new asymptotics for the structure and frequency of *linear* Kelvin waves on the sphere.

Next, we studied nonlinear Kelvin waves in the sphere. In the equatorial beta-plane approximation (large Lamb’s parameter), nonlinear Kelvin traveling waves can be approximated by applying the method of multiple scales to derive the Korteweg-deVries (KdV) equation (with mean currents) or the inviscid Burgers equation (neglecting mean currents) and then invoking the known analytic traveling waves of these models. On the sphere, it is impossible to derive a KdV model. However, a mixture of perturbation theory (for small amplitude) and a continuation/Fourier-Galerkin/Newton iteration algorithm (for larger amplitude) allows us to describe the nonlinear Kelvin wave on the sphere.

1.1 The Cnoidal/Corner/Breaking Scenario

The nonlinear Kelvin wave exhibits three regimes. For small amplitude, there are solitons and cnoidal waves whose latitude-and-depth structure is the same as for infinitesimal amplitude waves and whose dependence on longitude and time is described by the Korteweg-deVries (KdV) equation [2, 3]. For large amplitude, the wave steepens (“frontogenesis”) and then turns over (“breaking”). (Such a roll-over can be prevented by adding the right sort of damping as elaborated in [18], but it is possible the Kelvin wave becomes multi-valued in the same way as surface gravity waves breaking on a beach, or in a two-layer model.)

The largest traveling wave, which is the parameteric boundary between solitons and breaking, is a “corner wave” in which the wave crest has a discontinuous slope. The *JFM* article is focused on the structure and dynamics of the Kelvin corner wave using both perturbation theory and numerical computations and also on longitudinally-periodic traveling waves of lower amplitude.

Much is known about the CCB Scenario as reviewed in [9], [8], [10] and [21]. Pioneering work was done by Stokes [38], Ostrovsky [32] and Shrira [36, 37]. Near-corner waves are described through matched asymptotic expansions in [26] and [11].

Our recent *JFM* article is primarily about the corner wave. Before discussing it, we review the other two regimes.

CCB Scenario: Cnoidal/Corner/Breaking

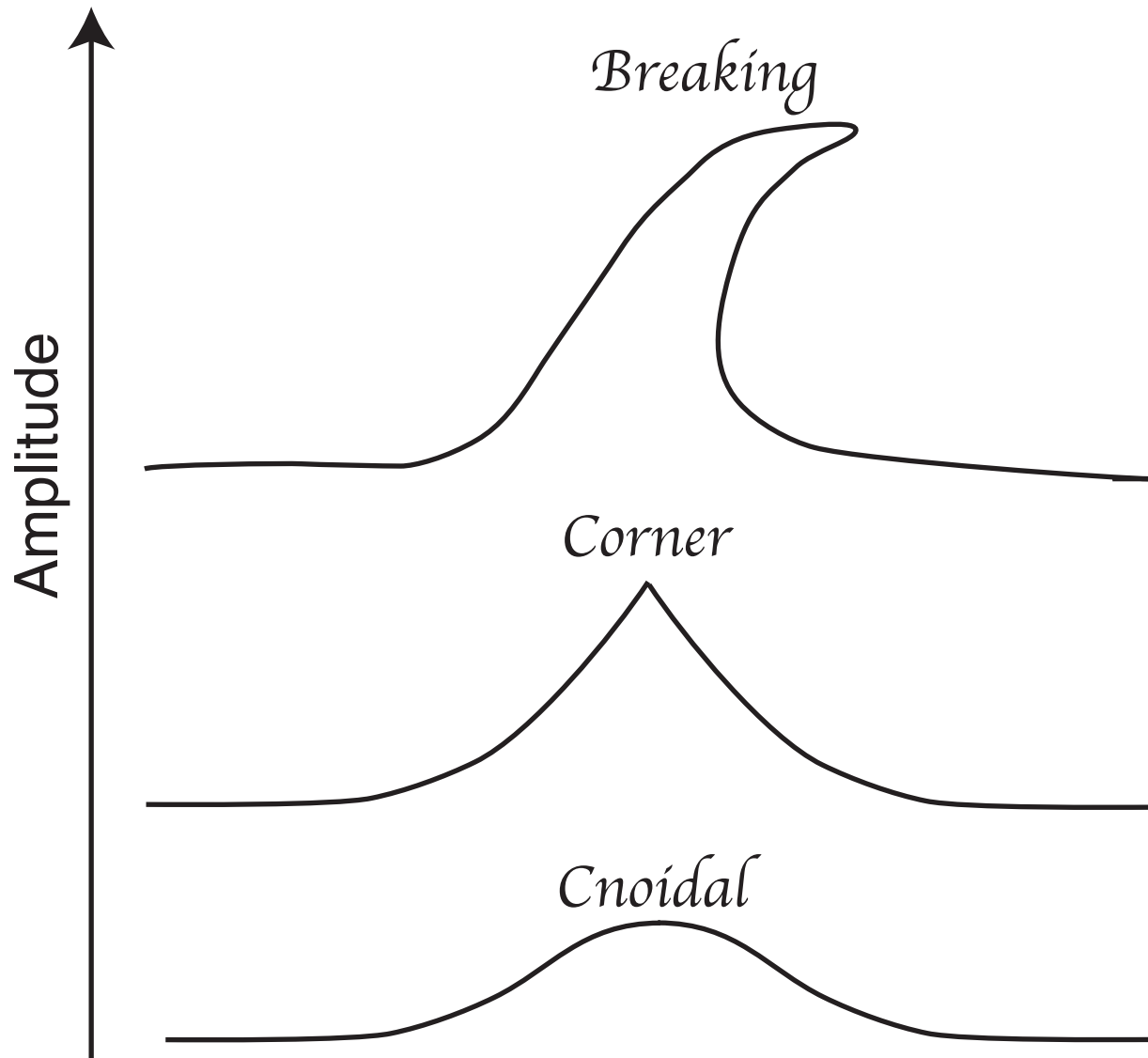


Figure 1: Three regimes for the Kelvin wave.

1.2 Frontogenesis and Breaking

Although we shall not compute initial-value solutions here, the statement that large amplitude Kelvin waves break is demonstrated in earlier articles by Long and Chen [24], Boyd [13, 9] and Boyd and Chen [17]. Kelvin breaking has been discussed by Boyd [1, 7], Ripa [34, 35] and Chen and Boyd [17], Fedorov and Melville [18] and Le Sommer, Reznik and Zeitlin [22].

On the equatorial beta-plane without mean currents, the linear Kelvin wave is completely nondispersive. Weakly nonlinear, nonresonant perturbation theory yields an approximation which has the same latitude-and-depth structure as the linear Kelvin wave, but the longitude-and-time dependence is described by the inviscid form of Burgers' equation [1, 34], also known as the One-Dimensional Advection equation.

This theory is a successful lowest-order approximation, but it predicts that the Kelvin front will be oriented north-south — that is, the maximum longitudinal gradients at each latitude will share a common meridian. In reality the Kelvin front curves westward away from the equator as illustrated in Fig. 2. Boyd [7] and Fedorov and Melville [18] showed the frontal curvature is due to resonance between the Kelvin wave and eastward-propagating gravity waves.

However, even the nonresonant theory has never been extended to the sphere, which remains a problem for the future.

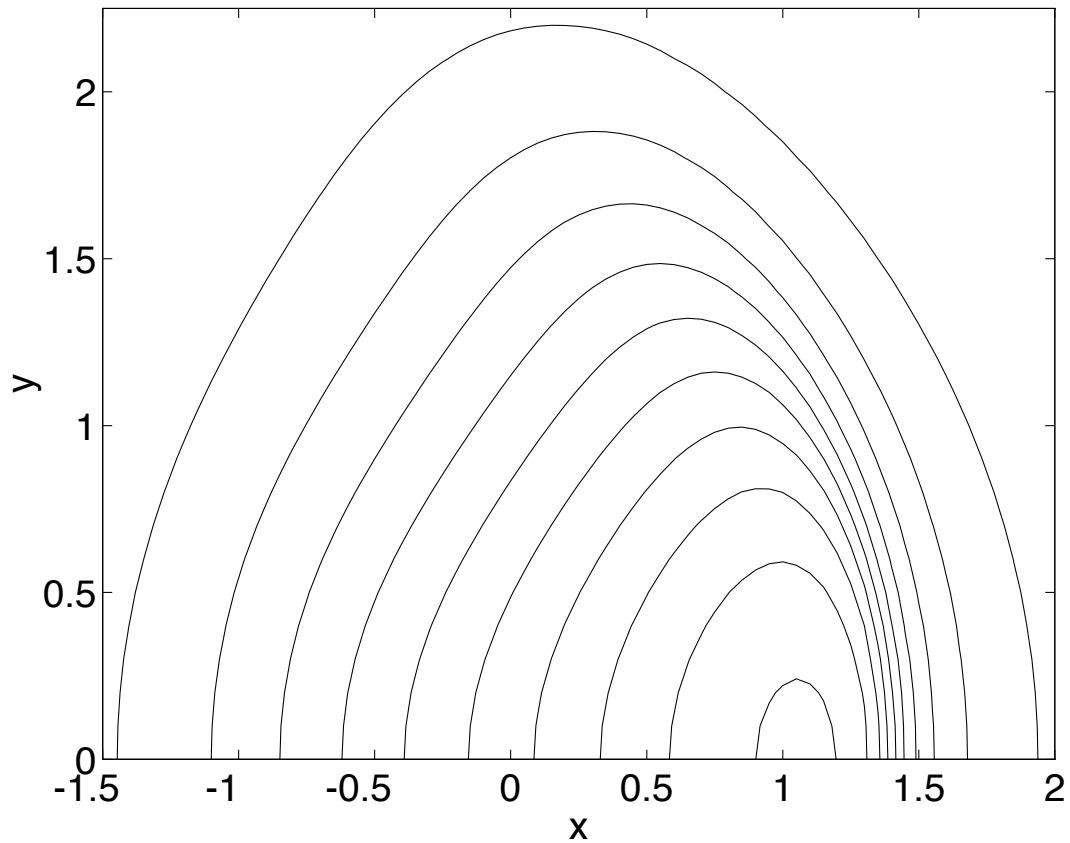


Figure 2: Contours of ϕ with the values $[0, .1, .2, .3, .4, .5, .6, .7, .8, 0.9, 1]$ for the Kelvin wave on the equatorial beta-plane . $u(x, y, 0) = \phi(x, y, 0) = \text{sech}^2(x) \exp(-0.5y^2)$. Only the northern hemisphere is shown because the wave is symmetric with respect to the equator, $y = 0$.

1.3 Kelvin Cnoidal Waves and Solitary Waves

Boyd showed that mean currents make the Kelvin wave dispersive even on the equatorial beta-plane [2]. To lowest order in perturbation theory, the approximation has the same latitude-and-depth structure as the linear Kelvin wave, but the longitude-and-time dependence is described by the Korteweg-deVries equation — identical to the One-Dimensional Advection equation except for an extra term proportional to the third derivative with respect to longitude. The KdV model predicts the existence of Kelvin solitary waves and cnoidal waves for small amplitude; instead of breaking, solitons and cnoidal waves form spontaneously. Initial value experiments confirm the KdV prediction (Fig. 3).

However, the KdV theory implies that the frequency of an infinitesimal amplitude Kelvin wave will be a parabola, growing as the square of the zonal wavenumber k without bound. In reality, numerical solutions for an infinitesimal Kelvin wave in a shear flow show that the Kelvin mode is *nondispersive* — not *infinitely dispersive* — in the “short wave limit” that $k \rightarrow \infty$ (Fig. 4.)

The KdV model fails for moderate amplitude. An open problem is to develop a small-amplitude theory that more realistically accounts for dispersion when the east-west scale is not small.

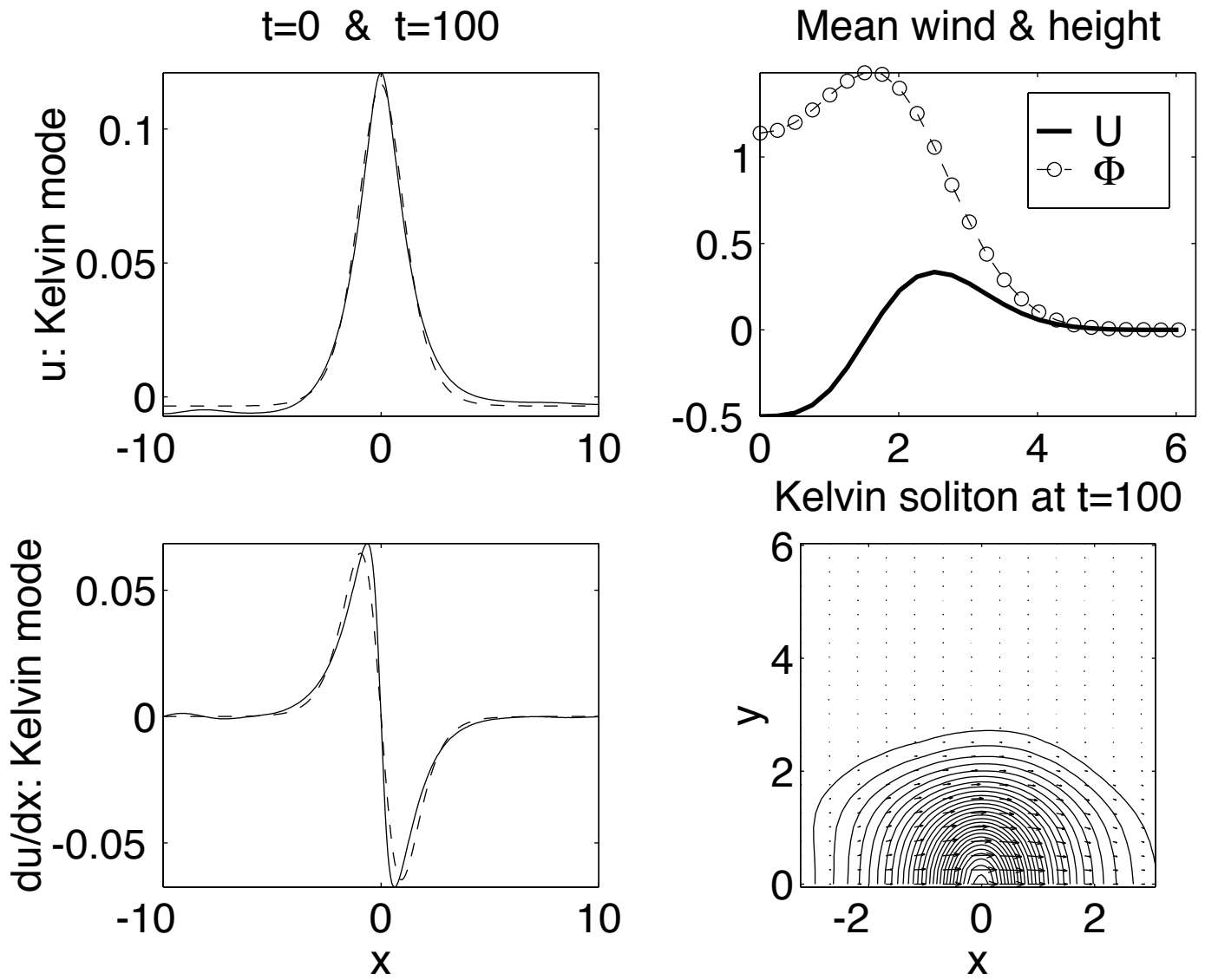


Figure 3: KELVIN SOLITON: left panels: Initial and final amplitude of the Kelvin mode. Upper right: mean flow & height. Lower right: contours of pressure/height and vector arrows. $u(x, y, 0) = \phi(x, y, 0) = 0.12\text{sech}^2(0.7x) - \text{constant}$.

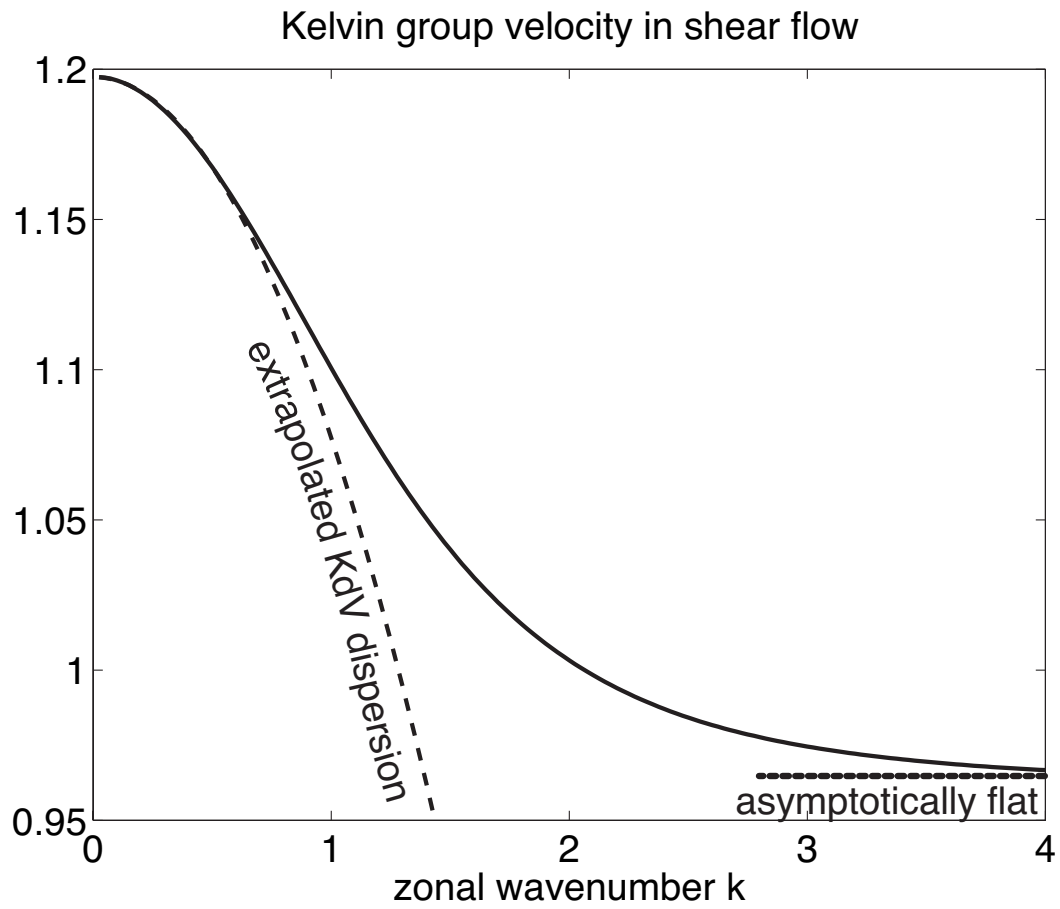


Figure 4: The solid line is the group velocity of linear Kelvin waves in a typical shear flow. The dashed line is a PARABOLA which is the KdV dispersion relation. Based on JPO paper (2005).

2 Parameters and a New Asymptotic Approximation for Linear Kelvin Waves

The Kelvin wave depends on two parameters. The zonal wavenumber s is always a positive integer. (The case of $s = 0$ is a nonpropagating mode which is not relevant here; note that we used a different symbol k for the zonal wavenumber in the previous section where the wavenumber was scaled in the usual equatorial way and not restricted to an integer.)

Lamb’s parameter ϵ is a nondimensional mean reciprocal depth which is explicitly

$$\epsilon = \frac{4\Omega^2 a^2}{gH} \quad (1)$$

where Ω is the angular frequency of the earth’s rotation in radians per second, a is the radius of the planet, H is the mean depth of the fluid, and g is the gravitational constant, which is 9.8 m/s^2 for earth. As explained in [16], [27] and [29], the shallow water equations can be profitably employed for continuously-stratified (rather than homogeneous) fluids if the depth H is interpreted as the “equivalent depth” of a given baroclinic mode. Thus, to describe all possible varieties of Kelvin waves in a three-dimensional stratified ocean or atmosphere, one needs to solve Laplace’s Tidal Equations for a very wide range of ϵ ranging from very small (for the “barotropic” or nearly-barotropic waves) to very large (for high order baroclinic modes) as illustrated in Table 1.

Table 1: Lamb’s Parameter

ϵ	Description	Source
0.012	External mode: Venus	Lindzen (1970)
6.5	External mode: Mars	Zurek (1976)
12.0	External mode: Earth (7.5 km equivalent depth)	Lindzen (1970)
2.6	Jupiter: simulate Galileo data	Williams (1996)
21.5	Jupiter	Williams (1996)
43.0	Jupiter	Williams (1996)
260	Jupiter	Williams (1996)
2600	Jupiter	Williams and Wilson (1988)
87,000	ocean: first baroclinic mode (1 m equiv. depth)	Moore & Philander (1977)
> 100,000	ocean: higher baroclinic modes	Moore & Philander (1977)

Fig. 5 shows the two-dimensional parameter space and its distinct regimes:

1. When s and ϵ are both small [bottom left in the figure], the Kelvin wave fills the entire globe from pole to pole.
2. When ϵ is large and much greater than s^2 , the Kelvin wave is well-approximated by the equatorial beta-plane [bottom right].

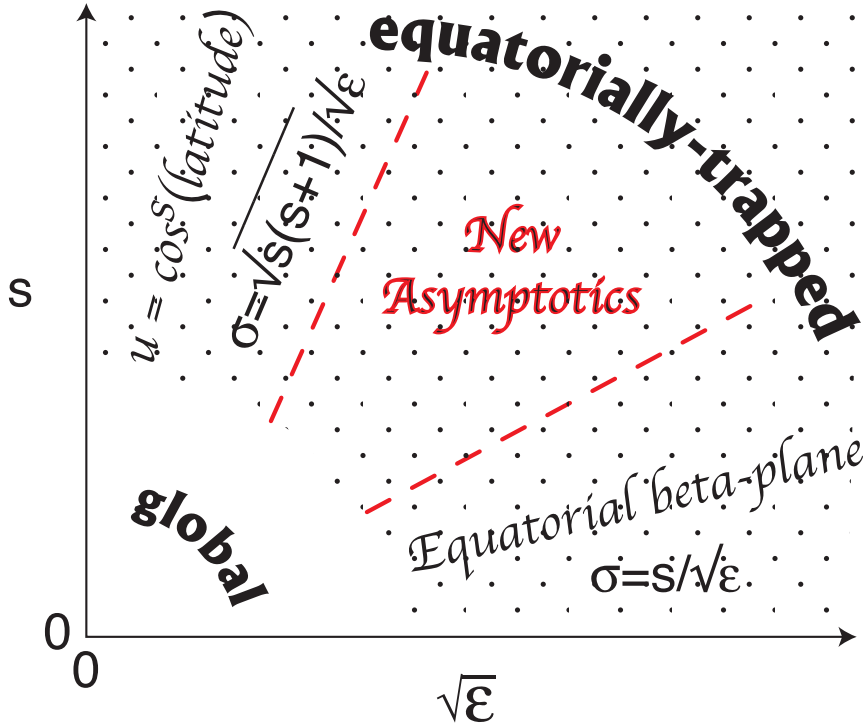


Figure 5: The Kelvin wave lives in a two-dimensional parameter space where the horizontal axis is the square root of Lamb's parameter ϵ and the vertical axis is the zonal wavenumber s . When s and ϵ are both small, the Kelvin wave is global. When $r \equiv \sqrt{s^2 + \epsilon}$ is large compared to one, the Kelvin wave is equatorially-trapped, proportional to $\exp(-(1/2)r\mu^2)$ where μ is the sine of latitude. The horizontal axis is $\sqrt{\epsilon}$ rather than ϵ itself so that r is just distance from the origin in this map of the parameter space. When ϵ is large and much greater than s^2 , the Kelvin wave is well-approximated by the equatorial beta-plane. When $s \gg \sqrt{\epsilon}$ (and not necessarily large), the velocity potential $\chi \approx \exp(is\lambda) P_s^s(\mu) = \cos^s(\text{latitude})$ where P_s^s is the usual associated Legendre function and the frequency $\sigma \approx \sqrt{s(s+1)}/\sqrt{\epsilon}$. The new asymptotic approximation derived in Boyd and Zhou (2007) fills the wedge-shaped gap between these two previously-known limits. However, the new approximation is not merely valid in this region, but is UNIFORMLY valid whenever either s or ϵ or both is large compared to one. This region of validity is shaded.

3. When $s \gg \sqrt{\epsilon}$ (and not necessarily large), the zonal velocity is $u \approx \exp(is\lambda) P_s^s(\mu)$ where P_s^s is the usual associated Legendre function and the frequency is $\sigma \approx \sqrt{s(s+1)}/\sqrt{\epsilon}$ [top right].
4. When the parameter combination $r \equiv \sqrt{s^2 + \epsilon}$ is large compared to one, the Kelvin wave is equatorially-trapped, proportional to $\exp(-(1/2)r\mu^2)$ where μ is the sine of latitude. [wedge between the dotted rays].

Boyd and Zhou derived a new asymptotic to describe *linear* Kelvin waves (in the absence of mean currents) to fill the gap between the three previously-known limits [15]. In the equatorial beta-plane approximation, all equatorial confinement comes from a term proportional to ϵ , independent of the zonal wavenumber s . Boyd showed twenty-five years ago [4] that on the sphere, equatorial confinement for *Rossby* waves is proportional to the parameter

$$r = \sqrt{s^2 + \epsilon} \tag{2}$$

Boyd and Zhou showed that the same is true for Kelvin waves. For $\epsilon = 0$, the barotropic case (infinite depth) in which ϵ provides no latitudinal trapping, Kelvin waves with $s \geq 5$ nonetheless have most of their amplitude concentrated in the tropics as illustrated in Fig. 6.

Fig. 7 shows that the new asymptotic approximation is much superior to the standard beta-plane approximation where the Boyd-Zhou approximation is

$$\phi \approx (1 - \mu^2)^{s/2} \exp(-(1/2) \left\{ \sqrt{\epsilon + s^2} - s \right\} \mu^2) \tag{3}$$

where $\mu = \sin(\text{latitude})$.

Barotropic Kelvin waves: $s=1, 2, \dots, 10$

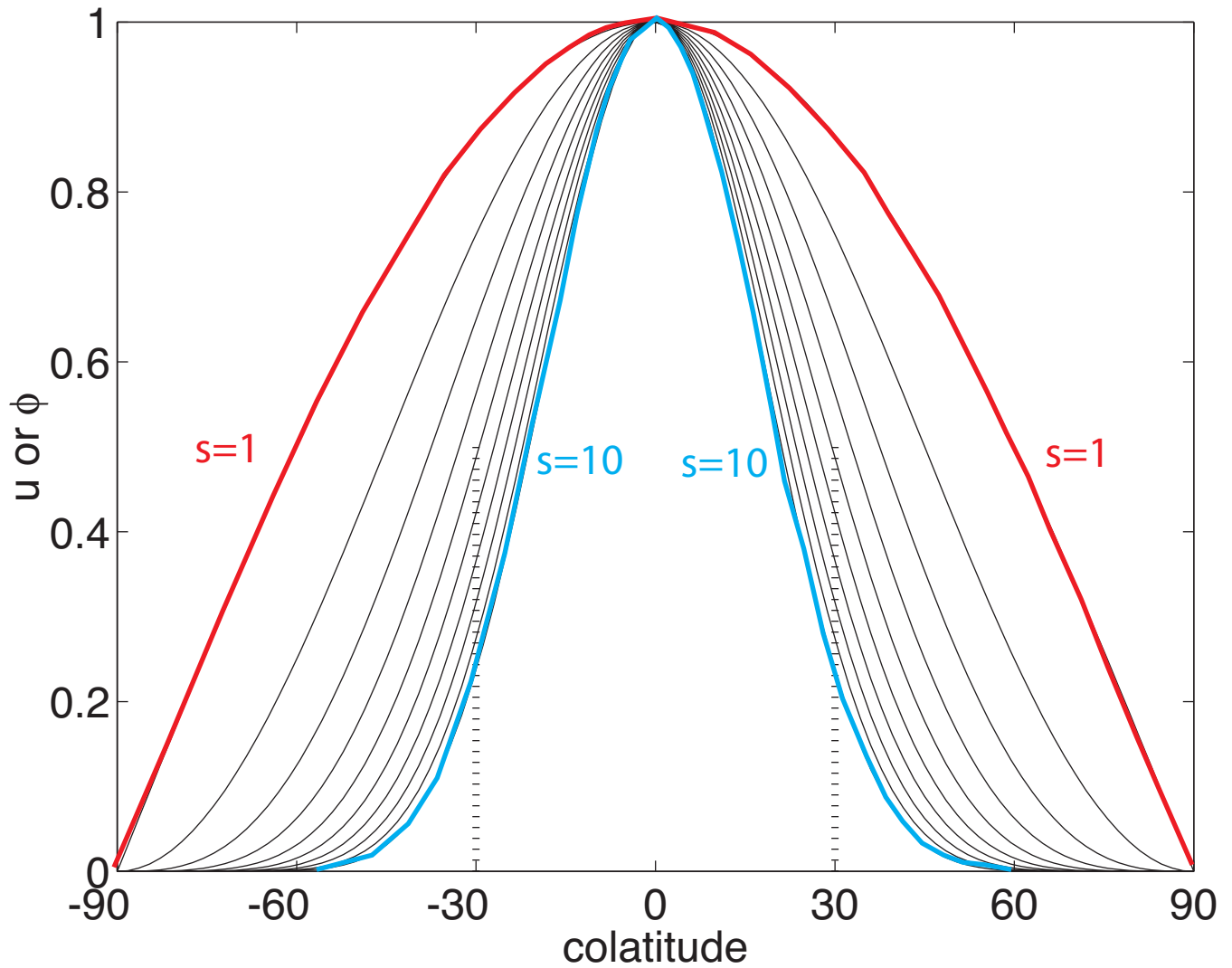


Figure 6: The latitudinal structure of u or ϕ (which are identical) for the lowest ten zonal wavenumbers s for $\epsilon = 0$ [barotropic waves]. $u = (1 - \mu^2)^{s/2}$. The widest curve is $s = 1$ and the waves become more and more narrow as s increases. The dotted curves are guidelines that show that the half-width of the wave is within the tropics ($|\text{latitude}| \leq 30^\circ$) for $s \geq 5$.

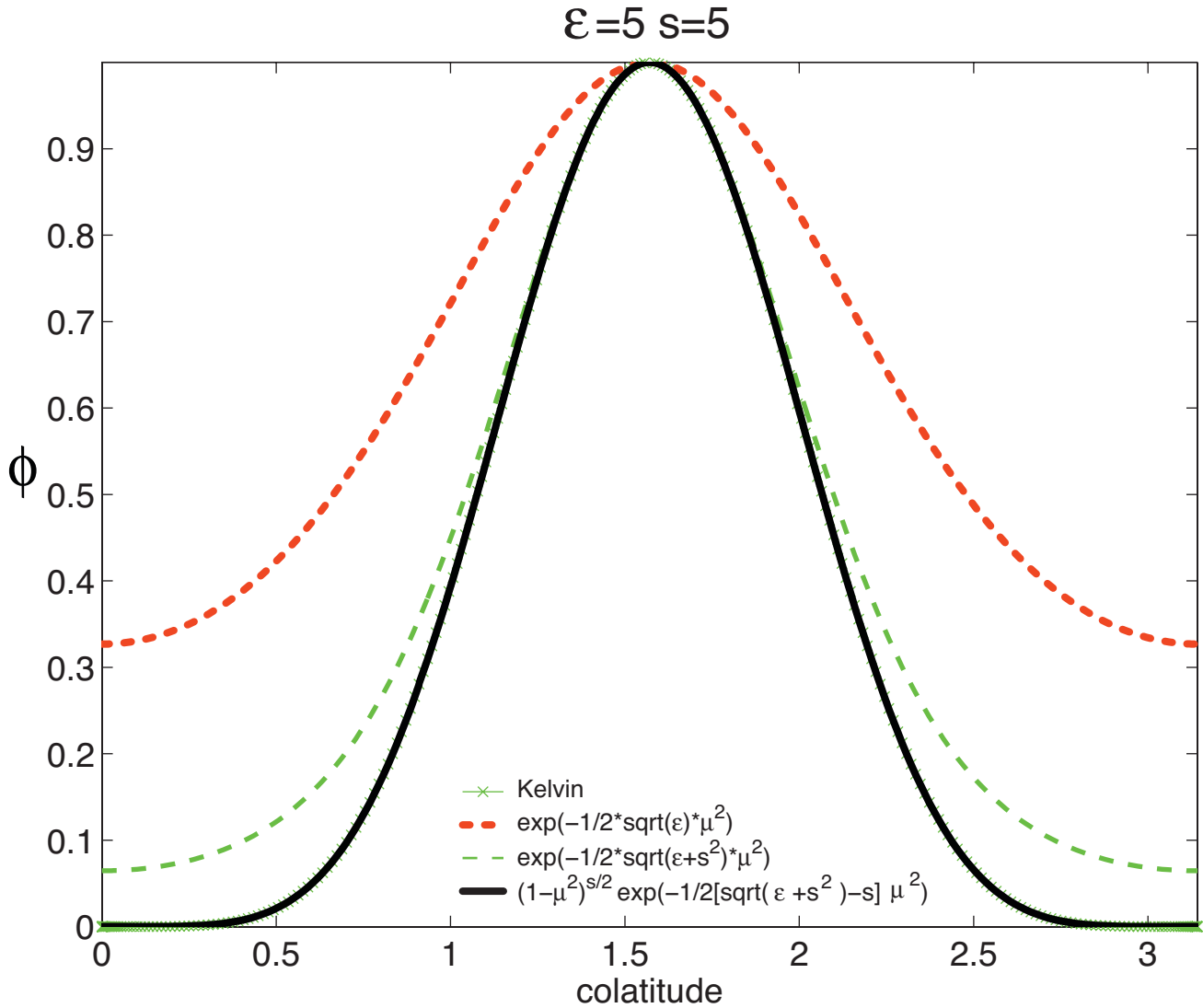


Figure 7: The thin curve with x's is the exact Kelvin mode for $s = 5$ and $\epsilon = 5$. The red dotted curve is the classical equatorial beta-plane approximation, $\phi \approx \exp(-1/2 \sqrt{\epsilon} \mu^2)$. The green dashed curve is the new asymptotic approximation without the $(1 - \mu^2)$ factor, $\phi \approx \exp(-1/2 \sqrt{\epsilon + s^2} \mu^2)$. The thick curve is the improved new asymptotic approximation, $\phi \approx (1 - \mu^2)^{s/2} \exp(-1/2 \{ \sqrt{\epsilon + s^2} - s \} \mu^2)$; this is graphically indistinguishable from the Kelvin wave.

3 Nonlinear Kelvin Traveling Waves

3.1 Traveling Wave Equations

Initial value experiments reported in [9] are consistent with the CCB Scenario. However, initial value experiments are a crude tool for traveling waves; although solitons form spontaneously and make dominate the evolved solution, a simple initial condition like a sine wave in longitude with the linear structure of a Kelvin wave will inevitably generate flows in which a few percent of the energy resides in non-Kelvin modes. In [14], we therefore calculated traveling waves directly by assuming that the dependence on longitude and time is solely through the combination $x \equiv \lambda - ct$. In the rest of this article, we summarize this work.

The usual nondimensionalization and derivation of the traveling wave equations is given in [14]. Define $\delta \equiv \sqrt{\epsilon}$. The shallow water equations become, without approximation,

$$(c(1 - \mu^2) - \delta u) \frac{\partial u}{\partial x} - \delta(1 - \mu^2)v \frac{\partial u}{\partial \mu} - (1 - \mu^2) \frac{\partial \phi}{\partial x} + \delta \mu(1 - \mu^2)v = 0 \quad (4)$$

$$(c(1 - \mu^2) - \delta u) \frac{\partial v}{\partial x} - \delta(1 - \mu^2)v \frac{\partial v}{\partial \mu} - (1 - \mu^2)^2 \frac{\partial \phi}{\partial \mu} - \delta \mu \{u^2 + v^2 + (1 - \mu^2)u\} = 0 \quad (5)$$

$$(c(1 - \mu^2) - \delta u) \frac{\partial \phi}{\partial x} - \delta(1 - \mu^2)v \frac{\partial \phi}{\partial \mu} - (1 + \delta \phi) \left(\frac{\partial u}{\partial x} + (1 - \mu^2) \frac{\partial v}{\partial \mu} \right) = 0 \quad (6)$$

where μ is the sine of latitude (cosine of colatitude) and u and v are the Margulus' velocities defined in [14]. This trio of equations is a nonlinear eigenvalue problem.

3.2 Omissions

Our study has two important restrictions:

1. Continuous vertical stratification is replaced by the shallow water/one-and-a-half layer model.
2. Mean currents are neglected.

The first restriction is not so bad. Ripa [35] and Marshall and Boyd [29] have studied the effects of vertical stratification on nonlinear equatorial waves. Nonlinearity is slightly weakened because in a continuously stratified model, an initial pulse in the first baroclinic mode no longer has nonlinear interactions that project solely on that mode, but instead some of the nonlinearity projects onto other modes. The barotropic mode is not equatorially-trapped, so energy in this mode leaks away from the tropics; an equatorial Kelvin soliton is “weakly nonlocal” in the parlance of Boyd’s monograph [6]. A future problem is to calculate this leakage into the barotropic mode, but it seems likely to be small.

The second restriction is more serious because the mean currents alter the dispersion of linear Kelvin waves; on the equatorial beta-plane, they are the sole source of dispersion.

3.3 Low-wavenumber Emphasis

We concentrate on *small* zonal wavenumbers; most explicit results are restricted to $s = 1$ and $s = 2$. As illustrated in [15], Kelvin waves of moderate and large s are *equatorial* rather than *global* modes and are therefore well-modeled by the equatorial beta-plane studies of previous work [7, 13]. The spherical effects are most pronounced for small s .

3.4 Perturbation Theory

Our first line of attack was perturbation theory. The simplest procedure would be a univariate expansion in the wave amplitude A . This fails because the linear Kelvin wave on the sphere, which is the lowest order of such an expansion, is known analytically only in the asymptotic limits $\epsilon \rightarrow 0$ and $\epsilon \rightarrow \infty$. We therefore employed a *double* expansion in both A and ϵ . It is not possible to do a similar expansion in $1/\epsilon$ because the linear Kelvin is nondispersive in the limit $\epsilon \rightarrow \infty$ (equatorial beta-plane).

The details are messy and will not be repeated here. The inhomogeneous ordinary differential equation which must be solved at each order is Legendre's equation. The good news is that the explicit solution can be found in closed form at each order.

The perturbation series is useful in two ways. First, it displays Kelvin cnoidal waves in explicit form. Second, it provides the initialization for the Newton-Galerkin-continuation numerical method.

3.5 Numerical Method

Perturbation theory is useful only for small amplitude. One can insert any arbitrary amplitude into the perturbation series, even for amplitudes far beyond the corner wave limit. Perturbation theory diverges at the corner wave, and probably for some amplitudes less than the corner wave.

It is a severe numerical challenge to track the entire branch of traveling waves up to and including the corner wave. In the corner wave limit, the wave will have a discontinuous x -derivative at the peak of the wave. The convergence rate of the Fourier coefficients of functions with a slope discontinuity is only $O(K^{-2})$, where K is the degree of the Fourier terms. By employing the Kepler mapping developed in [13], the convergence rate can be improved to $O(K^{-4})$ [14].

The traveling wave equations were expanded in Fourier series in latitude and the moving longitudinal coordinate $x = \lambda - ct$. The assumption that the traveling waves are symmetric in both latitude and longitude reduces the number of Fourier terms required by a factor of four, and also suppresses the translational degree of freedom.

The resulting system of nonlinear algebraic equations is solved by Newton's method. The traveling waves form a one-parameter family. To obtain a unique solution, it is necessary to impose one constraint on the Fourier basis. We chose

to fix ϕ_{00} , which is the equatorial height at the crest of the wave, $\phi(x = 0, \theta = \pi/2)$, as the amplitude parameter (though other choices are possible).

Newton's iteration requires an initialization or "first guess". Parameter continuation provided the required first guess. To trace a complete branch of solutions, we marched from small amplitude (where the initialization is provided by perturbation theory) to large amplitude while keeping all other parameters fixed. The continuation strategy is to march in small steps of the amplitude parameter. The computed solution for the j -th value of ϕ_{00} is used as the initialization for Newton's iteration to compute the Fourier coefficients \vec{a} for the $(j + 1)$ -st value of ϕ_{00} .

3.6 Detecting the Corner Wave

The branch of traveling waves ends abruptly at the corner wave: there are no solutions for larger amplitude. (Instead, all waves larger than the corner wave break.) The corner wave is a sort of anti-bifurcation point in the sense that no additional branches are born at the corner wave, but rather the branch simply dies [9].

A branch of solutions to a system of algebraic equations, however, can never simply stop. Consequently, the branch of solutions to the Galerkin discretization does not end at the corner wave, but *continues to larger amplitude*. The signature of the spurious solutions beyond the corner wave is that the Fourier series ceases to converge; the spurious "solutions" *oscillate* rapidly in space as typical of underresolved solutions.

Fig. 8 shows how the corner wave can be identified through a zoom plot of numerical solutions near the crest at $x = 0$. An unresolved issue is to obtain a less subjective quantitative criteria. See [13] for a fuller discussion.

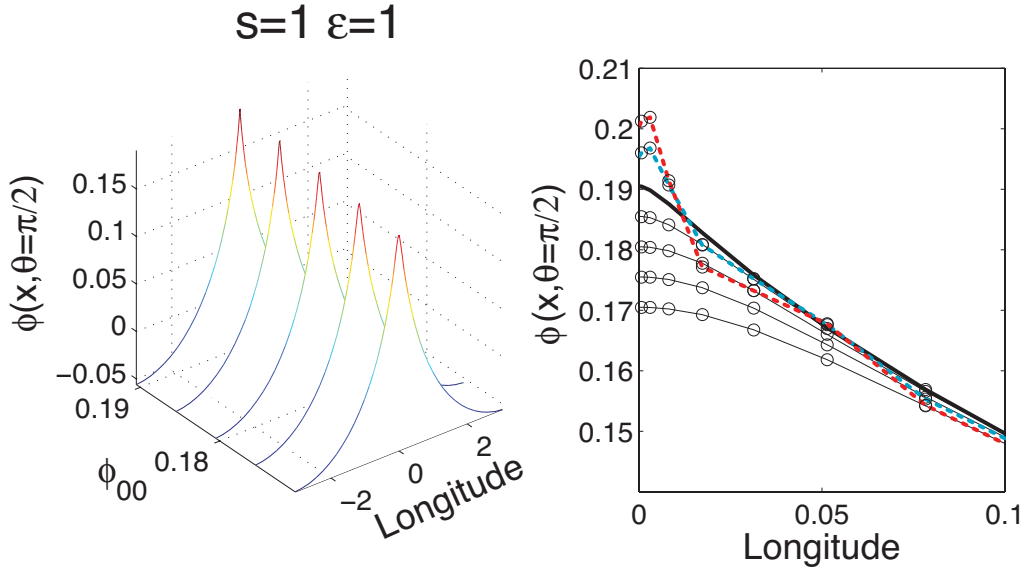


Figure 8: Traveling Kelvin wave solutions with $s = 1$ and $\epsilon = 1$. Left: equatorial section of ϕ for $\phi_{00} = 0.1705, 0.1755, 0.1805, 0.1855$ and 0.1905 , respectively. $\phi(x, \theta = \pi/2)$ steepens with the increasing ϕ_{00} . When $\phi_{00} = 0.1905$, $\phi(x, \pi/2)$ is the corner wave, discontinuous in its first derivative at the crest. Right: A zoom in plot of $\phi(x, \pi/2)$ with $\phi_{00} = 0.1755, 0.1805, 0.1855, 0.1905, 0.1955, 0.2005$. The heavy curve is for $\phi_{00} = 0.1905$. Note that this graph includes two values of ϕ_{00} larger than that of the corner wave (colored & dashed); these are unphysical as indicated by their rapid oscillations near $x = 0$. The interval in longitude is from 0 to 0.1, which is about 1.6% of the total width. (Note that the plot is in the physical longitudinal coordinate x ; the circles on each curve show the points of the grid, which is evenly spaced in the computational coordinate z , but very heavily concentrated by the Kepler mapping in x near $x = 0$.) This graph shows that the corner wave is easily distinguished by eye from near-corner waves with a zoom plot.

4 Spatial Structure of the Corner Wave

We computed steadily-propagating Kelvin waves of $s = 1$ (longitudinal period of 2π) and $s = 2$ (longitudinal period π) for various Lamb's parameter ϵ using the numerical methods described in the previous section.

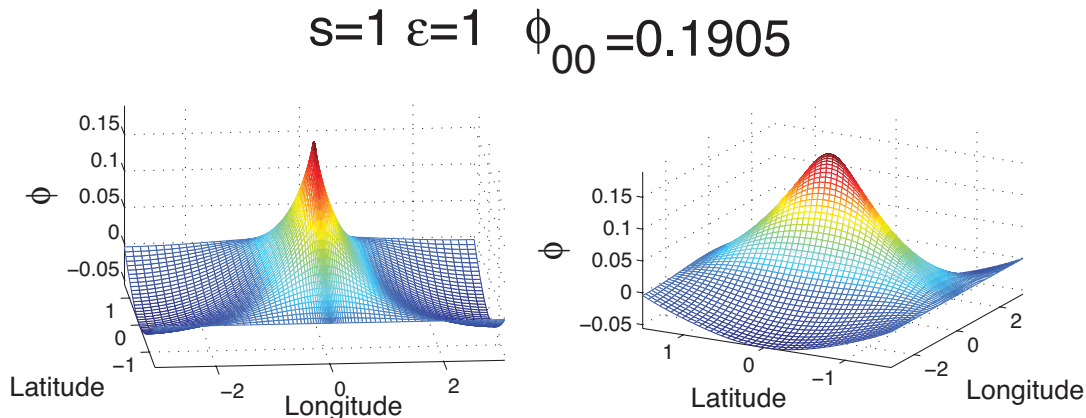


Figure 9: ϕ of the corner wave for $s = 1$ and $\epsilon = 1$ on sphere; left and right differ only in viewing angle. The peak value of ϕ_{00} is 0.1905. The comparison shows that only the LONGITUDINAL derivative is discontinuous at the peak.

Surface mesh plots ϕ for the corner wave limit are shown in Figure 9. One question is: Are *both* components of the gradient of ϕ discontinuous at the peak, or only one? We visually answered this question by plotting ϕ twice from different viewing angles. The left diagram shows that the longitudinal derivative is (at least visually) discontinuous. However, rotating the viewing angle by roughly a quarter-turn shows only a smooth, rounded crest: the north-south derivative shows no signs of discontinuity.

Figure 10 displays line graphs that, for two different values of ϵ , make the same point. In each, the solid curve is a longitudinal cross-section at the equator while the dashed curve shows $\phi(0, y)$. The x -derivative is discontinuous, but the latitudinal derivative is smooth.

Just as for infinitesimal amplitude Kelvin waves, u of the corner wave is graphically indistinguishable from ϕ and so is not plotted. The first derivative of the northward velocity v is everywhere continuous, so v is not plotted.

Another interesting question is how far does the slope discontinuity extend from the equator to the poles? To answer this question, we calculated $d\phi/dx$. Figure 11 shows ϕ_x at several latitudes, shown on the full longitudinal range at left and as a zoom plot on the right. A finite spectral series must always impose a truncation-dependent smoothing on a discontinuity. Even so, it is clear the slope rapidly diminishes away from the equator. It seems likely that the Kelvin wave is discontinuous only at the equator.

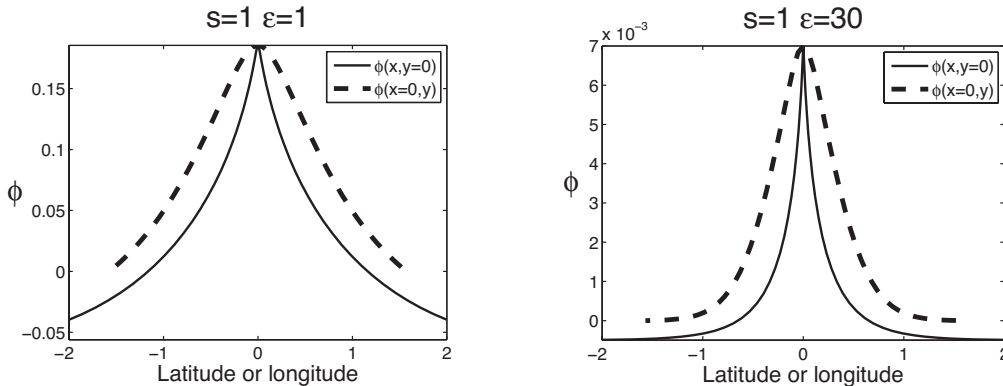


Figure 10: Profile of ϕ along the equator (solid) and the profile of ϕ at $x = 0$ as a function of latitude (dashed) for the corner wave for $s = 1$ for two different values of Lamb's parameter. [Left: $\epsilon = 1$. Right: $\epsilon = 30$.] The horizontal axis does doubly duty, being longitude for $\phi(x, \text{latitude} = 0)$ and latitude for $\phi(x = 0, \text{latitude})$. In both panels, the longitudinal derivative (solid) is clearly discontinuous at the crest whereas the north-south derivative shows not the slightest hint of non-smoothness.

Figure 12 compares $\phi(x, y = 0)$, normalized by dividing by ϕ_{00} , for many different ϵ . As ϵ increases, the corner wave becomes narrower and narrower in longitude. This trend is also evident by comparing the left and right panels of Fig. 10. Dispersion and the height of the corner wave both diminish rapidly as ϵ increases; it is remarkable that the corner wave becomes narrower, more focused in longitude, in this same limit. The latitudinal width, not shown, becomes narrower and narrower as captured by the equatorial beta-plane approximation, $\phi(x, \theta) \sim A(x) \exp(-\sqrt{\epsilon}(\theta - \pi/2)^2)$. However, the latitudinal width is controlled by *linear* dynamics whereas the longitudinal focusing is caused entirely by *nonlinearity*: when the amplitude is much smaller than the corner wave, the longitudinal structure of the Kelvin mode is approximately $\cos(s\lambda)$.

The graphs for $s = 2$ were so similar to those for $s = 1$ that they are omitted, but will appear in Zhou's forthcoming thesis. However, the maximum equatorial height $\phi_{00}(\epsilon)$ and phase speed $c(\epsilon)$ for the corner wave are discussed for both $s = 1$ and $s = 2$ in the next section.

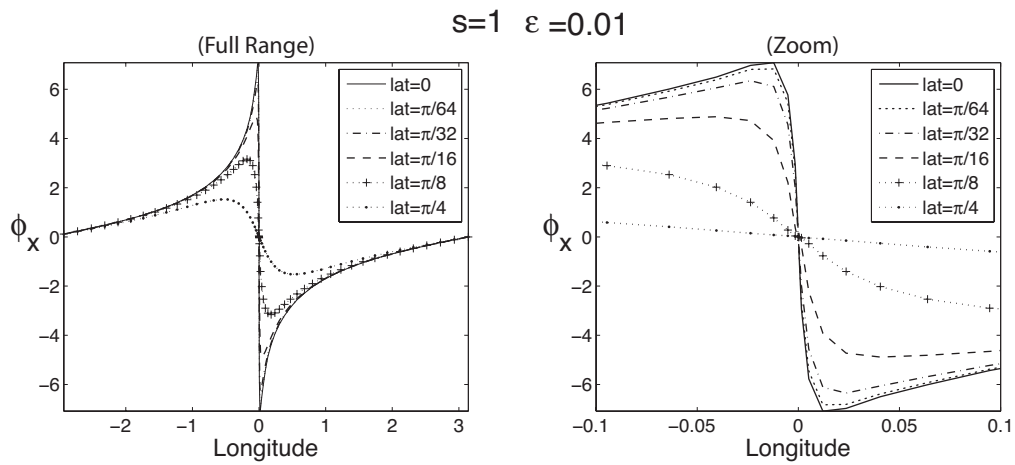


Figure 11: The derivative of ϕ of the corner wave solution of $s = 1$ and $\epsilon = 0.01$ case with respect to the longitude x . Left: ϕ_x at latitudes $0, \frac{\pi}{64}, \frac{\pi}{32}, \frac{\pi}{16}, \frac{\pi}{8}, \frac{\pi}{4}$, plotted on the full global domain. Right: same, but a zoom plot with a much smaller range.

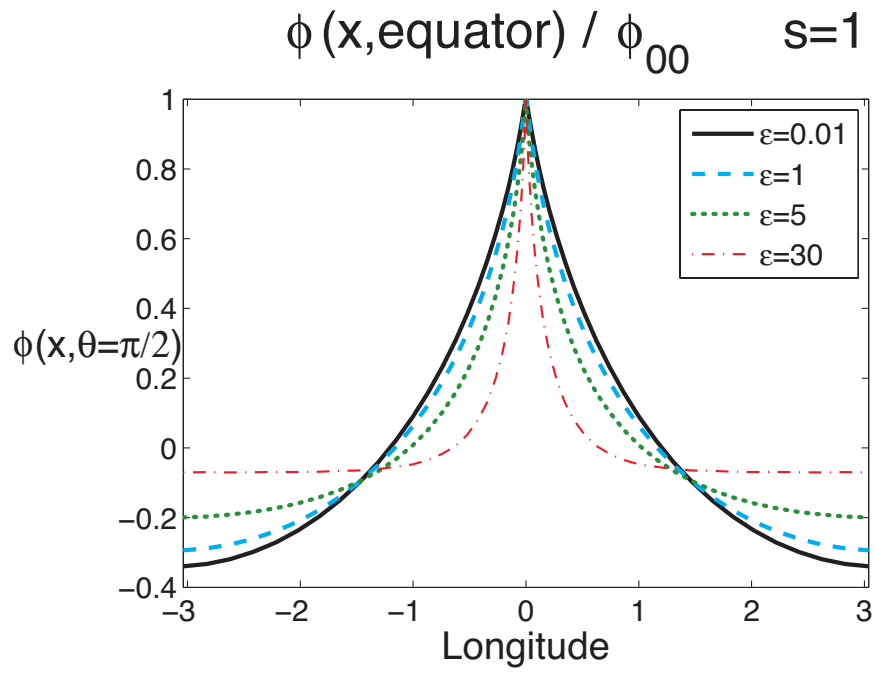


Figure 12: Normalized $\phi(x, \theta = \pi/2)$ [longitudinal section at the equator] of the corner wave solution of $s = 1$ and $\epsilon = 0.01, 1, 5, 30$. The profiles of $\phi(x, \theta = \pi/2)$ are scaled by their corresponding maxima, ϕ_{00} . The shape of ϕ at the equator becomes narrower and narrower as ϵ increases.

5 Variations of Phase Speed and Corner Height

The parameters of the corner wave for different ϵ are summarized in Table 2 [$s = 1$] and Table 3 [zonal wavenumber two]. From the table, we can see both ϕ_{00} and phase speed c decrease as ϵ increases. This is as expected: because the dispersion due to the earth's sphericity decreases rapidly with ϵ (as known from Longuet-Higgins' large ϵ asymptotic expansion of the linear phase speed), it is plausible that nonlinearity will overwhelm dispersion, giving breaking instead of traveling waves, at lower and lower values of the wave amplitude ϕ_{00} as $\epsilon \rightarrow \infty$.

ϵ	0.01	0.1	0.5	1	3	5	15	30
Phase speed c	1.4327	1.3792	1.3008	1.2551	1.1758	1.141	1.082	1.0572
ϕ_{00}	3.5	0.95	0.32	0.19	0.074	0.045	0.0145	0.0071
$(c^2 - 1)/(3\sqrt{\epsilon})$	3.5088	0.9510	0.3262	0.1918	0.0736	0.0450	0.0147	0.0072
$h_{00} \equiv \phi_{00}\sqrt{\epsilon}$	0.3500	0.3004	0.2263	0.1900	0.1282	0.1006	0.0562	0.0389

Table 2: Parameters in the corner wave limit for $s=1$ case

ϵ	0.01	0.1	0.5	1	3	5	15	30
Phase speed	1.2349	1.2169	1.1883	1.1698	1.1327	1.1135	1.0739	1.0537
ϕ_{00}	1.75	0.5	0.192	0.12	0.053	0.036	0.0129	0.0067
$(c^2 - 1)/(3\sqrt{\epsilon})$	1.7499	0.5069	0.1942	0.1228	0.0545	0.0358	0.0132	0.0067
$h_{00} \equiv \phi_{00}\sqrt{\epsilon}$	0.1750	0.1581	0.1358	0.1200	0.0918	0.0805	0.0500	0.0367

Table 3: Parameters in the corner wave limit for $s=2$ case

The tables also list the quantity

$$h_{00} \equiv \sqrt{\epsilon} \phi_{00} \quad (7)$$

This gives the maximum perturbative height of the Kelvin corner wave relative to the mean depth H , that is, the maximum perturbative height is $h_{00} H$ in meters. We have listed this quantity because it decreases more slowly with increasing ϵ than does ϕ_{00} itself.

Fig. 13 compares the equatorial height of the corner wave versus ϵ for both $s = 1$ and $s = 2$. The results are very similar for the two wavenumbers. As ϵ increases, the dispersion due to the sphericity of the earth decays very rapidly. Consequently, the height h_{00} of the corner wave diminishes very rapidly, too. On a log-log plot, a power law asymptotes to a straight line; the dashed guideline here suggests that $h_{00} \approx 0.2/\sqrt{\epsilon}$ for both wavenumbers one and two. The graph suggests that the corner wave maximum height is independent of zonal wavenumber s in the equatorial beta-plane limit that $\epsilon \rightarrow \infty$.

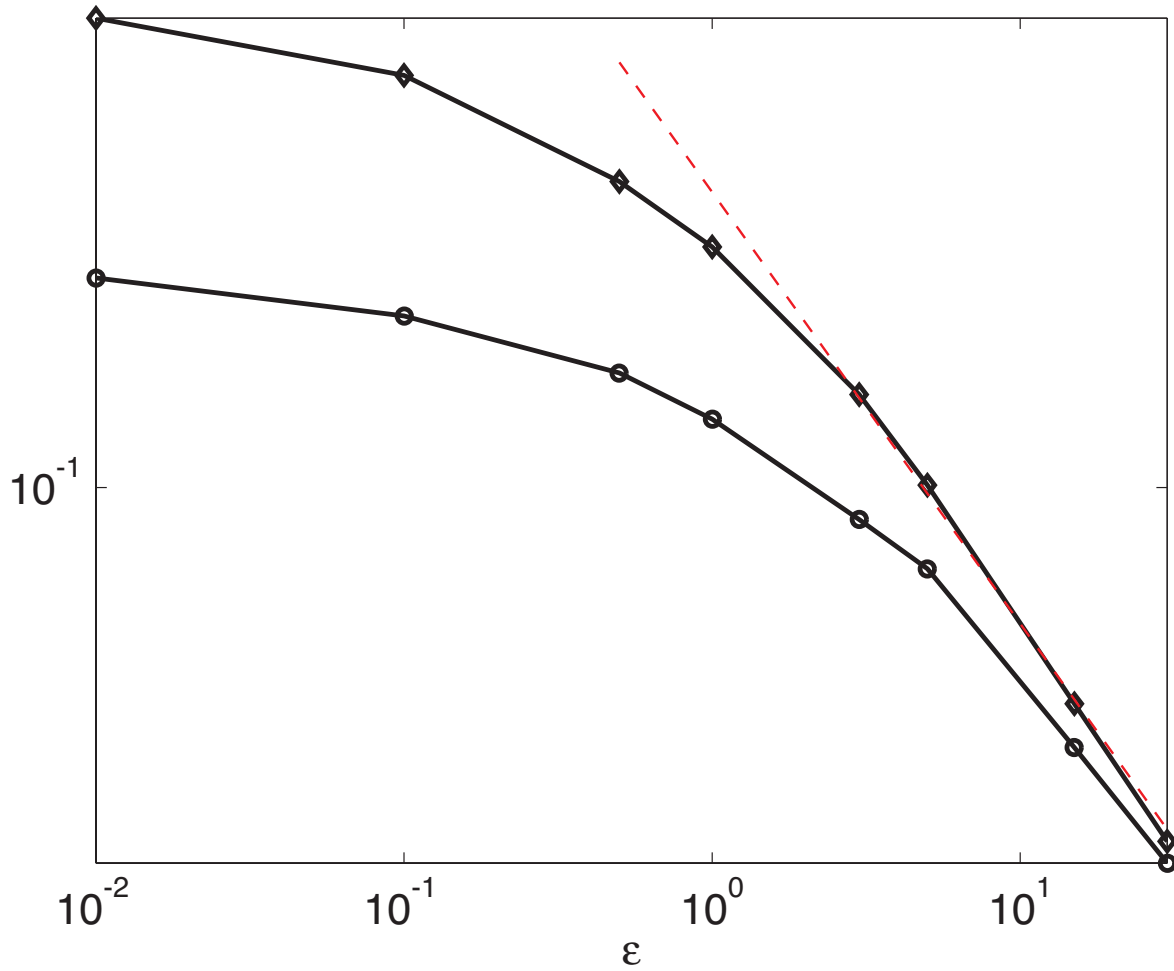


Figure 13: h_{00} of the corner waves of different ϵ for $s = 1$ [upper thick curve with diamonds] and $s = 2$ [lower thick curve with circles]. The dashed line on this log-log plot shows that h_{00} decays asymptotically proportional to $1/\sqrt{\epsilon}$ as $\epsilon \rightarrow \infty$.

The tables also show an interesting empirical relationship between the phase speed and maximum height of the corner wave:

$$\phi_{00} \approx \frac{c^2 - 1}{3\sqrt{\epsilon}} \quad (8)$$

By matching discontinuities in the x -derivatives of u and ϕ , we can derive the diagnostic relationship $(c - u_{00}\sqrt{\epsilon})^2 = 1 + h_{00}$ at the crest of the corner wave. (We thank a reviewer for suggesting this.) Unfortunately, it is not possible to extend this further: the rest of our study is based on perturbation series and computations.

6 Summary and Conclusions

The computations confirm the results of simplified models and equatorial beta-plane computations: the traveling waves of the Kelvin mode terminate in a corner wave of finite height. The amplitude of the corner wave diminishes very rapidly with ϵ when the mean flow is neglected. In the real ocean or atmosphere, our results for large ϵ are quantitatively suspect because the very weak dispersion due to spherical geometry would likely be overwhelmed by the stronger dispersion due to the mean zonal currents.

As ϵ increases, the longitudinal profile of the corner wave becomes very narrow whereas the corner waves for small ϵ span the whole equator.

In two space dimensions, slope discontinuities may take the form of a *cone* (with discontinuities in both x and y derivatives at the peak), a *crease* with a *curve* or *line* of discontinuous slope extending away from the equator into both hemispheres, or a *point* singularity in which only one derivative is discontinuous, and that only at a single point. All previous studies of corner waves have been limited to one horizontal dimension and therefore furnish no guidance. Although it is impossible to prove theorems through inexact numerical computations, our graphs strongly suggest that the third possibility is true of the Kelvin corner wave: the height and velocity fields are singular only at the peak, and only through a discontinuity in the direction of propagation, longitude.

Although we performed detailed computations only for zonal wavenumbers $s = 1$ and $s = 2$, there was so little qualitative difference that it appears that these conclusions are independent of zonal wavenumber s at least for small s . As illustrated in [15], Kelvin waves of moderate and large s are *equatorially-trapped*. Therefore, short Kelvin waves are well-described by the equatorial beta-plane theory and computations in [7, 13].

Our computations cannot exclude the possibility that there may be non-linear Kelvin branches which are not contiguous with small-amplitude, linear Kelvin waves. This is not a difficulty peculiar to Kelvin waves, but rather is a generic worry when computing the roots of any system of nonlinear algebraic or transcendental equations, whether resulting from the discretization of traveling waves or not; the peril of the “missed solution branch” is ubiquitous. How-

ever, no such additional branches have been detected in numerous initial-value experiments: all Kelvin modes bigger than the corresponding corner wave break.

Acknowledgments. This work was supported by the National Science Foundation through grants OCE OCE 0451951 and ATM 0723440.

References

- [1] J. P. BOYD, *The nonlinear equatorial Kelvin wave*, J. Phys. Oceanogr., 10 (1980), pp. 1–11.
- [2] ———, *Equatorial solitary waves, Part IV: Kelvin solitons in a shear flow*, Dyn. Atmos. Oceans, 8 (1984), pp. 173–184.
- [3] ———, *Equatorial solitary waves, Part 3: Westward-travelling modons*, J. Phys. Oceanogr., 15 (1985), pp. 46–54.
- [4] ———, *Barotropic equatorial waves: The non-uniformity of the equatorial beta-plane*, J. Atmos. Sci., 42 (1985), pp. 1965–1967.
- [5] ———, *Nonlinear equatorial waves*, in Nonlinear Topics of Ocean Physics: Fermi Summer School, Course LIX, A. R. Osborne, ed., North-Holland, Amsterdam, 1991, pp. 51–97.
- [6] ———, *Weakly Nonlocal Solitary Waves and Beyond-All-Orders Asymptotics: Generalized Solitons and Hyperasymptotic Perturbation Theory*, vol. 442 of Mathematics and Its Applications, Kluwer, Amsterdam, 1998. 608 pp.
- [7] ———, *High order models for the nonlinear shallow water wave equations on the equatorial beta-plane with application to Kelvin wave frontogenesis*, Dyn. Atmos. Oceans, 28 (1998), pp. 69–91.
- [8] ———, *A Legendre pseudospectral method for computing travelling waves with corners (slope discontinuities) in one space dimension with application to Whitham’s equation family*, J. Comput. Phys., 189 (2003), pp. 98–110.
- [9] ———, *The Cnoidal Wave/Corner Wave/Breaking Wave Scenario: a one-sided infinite-dimension bifurcation*, Math. Comput. Simulation, 69 (2005), pp. 235–242.
- [10] ———, *Near-corner waves of the Camassa-Holm equation*, Phys. Lett. A, 336 (2005), pp. 342–348.
- [11] ———, *Ostrovsky and Hunter’s generic wave equation for weakly dispersive short waves: analytical and numerical study of the parabolic and paraboloidal travelling waves (corner and near-corner waves)*, Eur. J. Appl. Math., 16 (2005), pp. 65–81.

- [12] ———, *The short-wave limit of linear equatorial Kelvin waves in a shear flow*, J. Phys. Oceanogr., 35 (2005), pp. 1138–1142.
- [13] ———, *Fourier pseudospectral method with Kepler mapping for travelling waves with discontinuous slope: Application to corner waves of the Ostrovsky-Hunter equation and equatorial Kelvin waves in the four-mode approximation*, Appl. Math. Comput., 177 (2006), pp. 289–299.
- [14] J. P. BOYD AND C. ZHOU, *Kelvin waves in the nonlinear shallow water equations on the sphere: Nonlinear travelling waves and the corner wave bifurcation*, J. Fluid Mech., 617 (2008), pp. 185–205.
- [15] ———, *Uniform asymptotics for the linear Kelvin wave in spherical geometry*, J. Atmos. Sci., 65 (2008), pp. 655–660.
- [16] S. CHAPMAN AND R. S. LINDZEN, *Atmospheric Tides*, D. Reidel, Dordrecht, Holland, 1970. 200 pp.
- [17] G. Y. CHEN AND J. P. BOYD, *Nonlinear wave packets of equatorial Kelvin waves*, Geophys. Astrophys. Fluid Dyn., 96 (2002), pp. 357–379.
- [18] A. V. FEDOROV AND W. K. MELVILLE, *Kelvin fronts on the equatorial thermocline*, J. Phys. Oceanogr., 30 (2000), pp. 1692–1705.
- [19] A. E. GILL, *Atmosphere-Ocean Dynamics*, vol. 30 of International Geophysics, Academic, Boston, 1982.
- [20] R. J. GREATBATCH, *Kelvin wave fronts, Rossby solitary waves and nonlinear spinup of the equatorial oceans*, J. Geophys. Res., 90 (1985), pp. 9097–9107.
- [21] R. H. J. GRIMSHAW, L. A. OSTROVSKY, V. I. SHRIRA, AND Y. A. STEPANYANTS, *Long nonlinear surface and internal gravity waves in a rotating ocean*, Surveys in Geophysics, 19 (1998), pp. 289–338.
- [22] J. LE SOMMER, G. M. REZNIK, AND V. ZEITLIN, *Nonlinear geostrophic adjustment of long-wave disturbances in the shallow-water model on the equatorial beta-plane*, J. Fluid Mech., 515 (2004), pp. 135–170.
- [23] R. S. LINDZEN, *The application of terrestrial atmospheric tidal theory to Venus and Mars*, J. Atmos. Sci., 27 (1970), pp. 536–549.
- [24] B. LONG AND P. CHANG, *Propagation of an equatorial Kelvin wave in a varying thermocline*, J. Phys. Oceanogr., 20 (1990), pp. 1826–1841.
- [25] M. S. LONGUET-HIGGINS, *The eigenfunctions of Laplace’s tidal equation over a sphere*, Phil. Trans. Royal Society of London, Series A, 262 (1968), pp. 511–607.
- [26] M. S. LONGUET-HIGGINS AND M. J. H. FOX, *Asymptotic theory for the almost-highest wave*, J. Fluid Mech., 317 (1996), pp. 1–19.

- [27] A. MAJDA, *Introduction to PDEs and Waves for the Atmosphere and Ocean*, vol. 9 of Courant Lecture Notes, American Mathematical Society, Providence, Rhode Island, 2003.
- [28] A. J. MAJDA, R. R. ROSALES, E. G. TABAK, AND C. V. TURNER, *Interaction of large-scale equatorial waves and dispersion of Kelvin waves through topographic resonances*, J. Atmos. Sci., 56 (1999), pp. 4118–4133.
- [29] H. G. MARSHALL AND J. P. BOYD, *Solitons in a continuously stratified equatorial ocean*, J. Phys. Oceanogr., 17 (1987), pp. 1016–1031.
- [30] P. A. MILEWSKI AND E. G. TABAK, *A reduced model for nonlinear dispersive waves in a rotating environment*, Geophys. Astrophys. Fluid Dynamics, 90 (1999), pp. 139–159.
- [31] D. W. MOORE AND S. G. H. PHILANDER, *Modelling of the tropical oceanic circulation*, in The Sea, E. D. Goldberg, ed., no. 6 in The Sea, Wiley, New York, 1977, pp. 319–361.
- [32] L. A. OSTROVSKY, *Nonlinear internal waves in a rotation ocean*, Oceanology, 18 (1978), pp. 181–191.
- [33] J. PEDLOSKY, *Geophysical Fluid Dynamics*, Springer-Verlag, New York, 2d ed., 1987.
- [34] P. RIPA, *Nonlinear wave-wave interactions in a one-layer reduced-gravity model on the equatorial beta-plane*, J. Phys. Oceanogr., 12 (1982), pp. 97–111.
- [35] ———, *Nonlinear effects in the propagation of Kelvin pulses across the Pacific Ocean*, in Advances in Nonlinear Waves, L. Debnath, ed., Pitman, New York, 1985, pp. 43–56.
- [36] V. I. SHRIRA, *Propagation of long nonlinear waves in a layer of rotating fluid*, Ivestiya Atm. Oceanic Phys., 17 (1981), pp. 76–81.
- [37] ———, *On long strongly nonlinear waves in a rotating ocean*, Ivestiya Atm. Oceanic Phys., 22 (1986), pp. 298–305.
- [38] G. G. STOKES, *On the theory of oscillatory waves*, Camb. Trans., 8 (1847), pp. 441–473. Also published in vol. 1 of *Mathematical and Physical Papers* (Cambridge University Press, Cambridge, 1880), pgs. 197–229.
- [39] G. P. WILLIAMS, *Jovian dynamics. Part I. Vortex stability, structure and genesis*, J. Atmos. Sci., 53 (1996), pp. 2685–2734.
- [40] G. P. WILLIAMS AND R. J. WILSON, *The stability and genesis of Rossby vortices*, J. Atmos. Sci., 45 (1988), pp. 207–249.
- [41] R. W. ZUREK, *Diurnal tide in Martian atmosphere*, J. Atmos. Sci., 33 (1976), pp. 321–337.